

CPI-1189 prevents apoptosis and reduces glial fibrillary acidic protein immunostaining in a TNF- α infusion model for AIDS dementia complex

Kimberly B Bjugstad¹, William D Flitter⁴, William A Garland⁴, Rex M Philpot¹, Cheryl L Kirstein¹ and Gary W Arendash^{*,2,3}

¹Department of Psychology, University of South Florida, 4202 East Fowler Avenue, Tampa, FL 33620, USA; ²Department of Biology, University of South Florida, 4202 East Fowler Avenue, Tampa, FL 33620, USA; ³James A Haley Veteran's Hospital, Tampa, FL 33612, USA and ⁴Centaur Pharmaceuticals, Inc., Sunnyvale, CA 94086, USA

AIDS dementia complex (ADC) is characterized by increased apoptosis, gliosis, and oxidative stress in the CNS, as well as a compromised blood-brain barrier. TNF- α has been shown to be elevated in AIDS dementia complex brains and may contribute to AIDS dementia complex. To model elevated TNF- α in AIDS dementia complex, TNF- α was infused ICV bilaterally into rats for 3 days. TNF- α treatment increased apoptosis around the infusion site and selectively in the septum and corpus callosum. Co-administration of the synthetic antioxidant CPI-1189 prevented TNF- α induced apoptosis. Both TNF- α and CPI-1189 treatment suppressed glial fibrillary acidic protein (GFAP) staining at the infusion site. TNF- α did not significantly affect the integrity of the blood-brain barrier, but CPI-1189 treatment increased blood-brain barrier integrity at the infusion site. No effect of TNF- α or CPI-1189 treatment was found on measures of oxidative stress. These results support TNF- α as a key agent for increasing apoptosis in AIDS dementia complex. Additionally, CPI-1189 treatment may protect against TNF- α induced apoptosis and astrogliosis in AIDS dementia complex. Lastly, the toxic effect of TNF- α and the protective effect of CPI-1189 may not be mediated primarily through manipulation of classic reactive oxygen species. *Journal of NeuroVirology* (2000) 6, 478–491.

Keywords: antioxidant; apoptosis; inflammation; tumor necrosis factor- α

Introduction

AIDS dementia complex (ADC) is a term that has been used to classify the behavioral and neuropathological changes due to HIV infection in the CNS in the absence of any co-existing CNS infections. Behaviorally, ADC is characterized by diminished cognitive, motor, and social skills (Maruff *et al*, 1994; Tross *et al*, 1988; Navia *et al*, 1986a). Neuropathologically, the ADC brain exhibits ventricular enlargement, diffuse myelin pallor, and generalized brain atrophy (Aylward *et al*, 1995; Artigas *et al*, 1994; Navia *et al*, 1986b). A widening of sulci in the frontal, parietal, and temporal cortices has also been found (Navia *et al*, 1986b; Gelman *et al*, 1992), as has a decrease in volume of

basal ganglia structures (caudate nucleus, putamen, and globus pallidus) (Aylward *et al*, 1993; Hestad *et al*, 1993; Dal Pan *et al*, 1992). Brain atrophy and ventricular enlargement both correlate with the cognitive impairment seen in ADC (Hestad *et al*, 1993; Jacobsen *et al*, 1989).

There are also cellular changes that occur in ADC brains, both to neurons and to supportive glial cells. Compared to HIV+ patients without CNS involvement, there are greater numbers of apoptotic cells in neocortical grey and subcortical grey matter, as well as in white matter of HIV+ patients having CNS involvement (An *et al*, 1996; Dickson *et al*, 1995; Petito *et al*, 1995). In addition to increased apoptosis, the neocortex and basal ganglia in particular show an increase in astrogliosis and microgliosis (Masliah *et al*, 1992; Glass *et al*, 1995). There is also evidence that HIV infection disrupts the blood-brain barrier. Using immunohistochemical staining for serum proteins, such as

*Correspondence: GW Arendash

Received 14 December 1999; revised 22 March 2000; accepted 8 June 2000

immunoglobulin G (IgG), increased levels of staining have been seen in the neocortex, basal ganglia, and white matter of AIDS brains (Power *et al*, 1993; Petitto *et al*, 1992).

Since the primary hosts of HIV infection in the brain are microglia/macrophages, the CNS cell loss, the brain atrophy, and ultimately the behavioral changes of ADC result from secondary effects of brain HIV infection (Glass *et al*, 1995; Takahashi *et al*, 1996; Smith *et al*, 1990). These secondary effects are suspected to involve enhanced CNS levels of glial-released inflammatory cytokines – most notably tumor necrosis factor α (TNF- α) – which can potentiate the inflammatory response and are neurotoxic via apoptotic and free radical mechanisms (Pace *et al*, 1995; Shoji *et al*, 1995; Streit and Kincaid-Colton, 1995; Greenspan and Aruoma, 1994; Tracey and Cerami, 1993; Odeh *et al*, 1990). TNF- α is suspected to be a primary cytokine through which brain damage occurs in ADC because: (1) ADC brains show increased TNF- α mRNA and protein, with the highest levels found in areas showing the greatest HIV infection (Glass *et al*, 1993, 1995; Wiley *et al*, 1986); (2) TNF- α mRNA and the number of TNF-positively stained cells in ADC brains are correlated with the level of cognitive impairment in HIV-infected patients (Seilhean *et al*, 1997; Wesselingh *et al*, 1993); and (3) TNF- α may enhance HIV replication (Wilt *et al*, 1995; Peterson *et al*, 1992; Folks *et al*, 1989). Previously we found that by mimicking the increased levels of brain TNF- α seen in ADC, a TNF- α i.c.v. infused rat has cognitive deficits and correlating ventricular enlargement similar to ADC (Bjugstad *et al*, 1998).

Because ADC may not evolve directly out of HIV CNS infection, but rather from secondary effects of the infection, such as neuroinflammation and ensuing free radical formation, drug intervention for ADC should be directed at reducing those effects. In our TNF- α CNS infused rat model of ADC, we found that co-administration of the novel synthetic compound, 4-acetamido-N-tert-butylbenzamide (CPI-1189) prevented all of the TNF- α effects analyzed. CPI-1189 is structurally related to the spin-trap nitron antioxidant, α -Phenyl-tert-butyl-nitron (PBN); however, CPI-1189 has an improved pharmacokinetic and bioavailability profile (unpublished observation, Centaur Pharmaceuticals, Inc.). Our earlier study showed that co-administration of CPI-1189 improved the learning and memory abilities of TNF- α infused animals to the level of controls, blocked TNF- α induced weight loss and prevented the ventricular enlargement seen in TNF- α infused rats (Bjugstad *et al*, 1998).

The present study was designed to further develop our rat TNF- α infusion model of ADC and to characterize the potential CNS of CPI-1189 by determining the effects of intracerebral TNF- α infusions on: (1) the frequency of apoptosis in specific brain areas that are shown to be involved

in HIV infection of the CNS; (2) the induction of astrocytosis in these same brain areas via GFAP staining; (3) the integrity of the blood-brain barrier via IgG staining; and (4) measures of brain oxyradical production and oxidative damage, via salicylate hydroxylation and TBAR formation, respectively. In addition, this study explored a shorter treatment time point than our previous study as cell culture studies show that TNF- α induced apoptosis can peak as early as 48–72 h after exposure (Talley *et al*, 1995; Selmaj *et al*, 1991a). Thus, in order to augment the evaluation of TNF- α induced apoptosis, i.c.v. and oral treatments were given for 3 days, compared to 7 days in the previous study. The ability of CPI-1189 to prevent any TNF- α induced neuropathologic and neurochemical effects was also evaluated in the context of this compound's potential usefulness to treat ADC.

Results

Apoptosis analysis

Figure 1 shows the total effect of TNF- α and CPI-1189 treatments on apoptosis around the infusion site. The total effect was calculated by adding the number of apoptotic cells from the neocortex, basal ganglia, and corpus callosum. After 3 days of treatment, TNF- α increased apoptosis surrounding the infusion site, as indicated by a significantly greater number of apoptotic cells seen in the TNF/Veh treated group compared to the Sal/Veh treated group ($P \leq 0.005$). In addition, CPI-1189 prevented the TNF- α induced apoptosis because the TNF/CPI1 treated group had significantly less apoptosis than

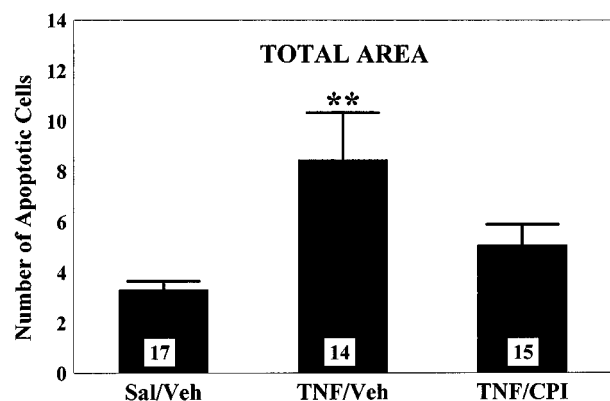


Figure 1 Total number of apoptotic cells surrounding the infusion site as a result of intracerebroventricular TNF- α infusions with or without oral CPI-1189 treatment for 3 days. The number of apoptotic cells found in the neocortex, corpus callosum, and basal ganglia were added together for each infusion site. Data represent mean \pm s.e.m., and the number at the base of each bar indicates the number of infusion sites for that group. The abscissa indicates the i.c.v./oral treatment of the groups. **Indicates significantly greater than both Sal/Veh and TNF/CPI. Significance at $P \leq 0.05$.

the TNF/Veh treated group ($P \leq 0.05$) and was not significantly different from the Sal/Veh group.

Figure 2 shows apoptotic cells in the neocortical tissue near the cannula tract stained for apoptosis. The neocortical tissue of the Sal/Veh treated animal (Figure 2A) and TNF/CPI treated animal (Figure 2C) is clear of apoptosis in the neocortical parenchyma, while the animal treated with TNF- α alone, shows several apoptotic cells (Figure 2B). An enlargement of an apoptotic cell can be seen in the inset of Figure 2B.

TNF- α infusions also affected specific areas in terms of apoptosis. While no significant differences were found in the neocortex between treatment groups (Figure 3A), analysis of apoptosis in the corpus callosum revealed that TNF- α induced apoptosis in this area, as seen by significantly more apoptosis in the TNF/Veh treated group compared to the Sal/Veh treated group ($P \leq 0.03$). This TNF- α induced apoptosis in the corpus callosum was prevented by co-administration of CPI-1189, as indicated by significantly less apoptosis in TNF/CPI treated animals compared to TNF/Veh treated animals ($P \leq 0.03$; Figure 3B) and no difference between TNF/CPI and Sal/Veh treatment groups.

As in the neocortex, there was no significant difference in apoptosis in the basal ganglia between groups after 3 days of treatment (Figure 3C). By contrast, there was a significant difference in apoptosis between groups in the septum (Figure 3D). TNF- α induced apoptosis in the septum, as indicated by significantly more apoptosis in the TNF/Veh treated group compared to Sal/Veh ($P < 0.03$, one-tail test). Co-treatment with CPI-1189 prevented apoptosis induced by TNF- α in the septum, as TNF/CPI treated animals were significantly different from TNF/Veh treated animals ($P \leq 0.03$) but were not different from Sal/Veh treated control animals.

Glial fibrillary acidic protein analysis

Analysis of overall effects of TNF- α infusion in the region surrounding the infusion site was analyzed by calculating the average percent area of GFAP staining from the neocortex, basal ganglia, and corpus callosum. This average per cent indicates that in the overall infusion area, treatment with TNF- α , and especially with CPI-1189, decreased GFAP staining (Figure 4). The TNF/Veh treated group had a significantly lower per cent area of GFAP staining compared to Sal/Veh controls ($P \leq 0.02$). Co-administration of CPI-1189 produced a greater suppression of GFAP staining than TNF- α alone, as TNF/CPI treated animals had a significantly lower per cent of GFAP stained area than Sal/Veh and TNF/Veh treated animals ($P \leq 0.00005$ and $P \leq 0.03$ one tail test, respectively). Results in the neocortical tissue resemble that which was found for the total area (Figure 5A). Treatment with TNF- α and

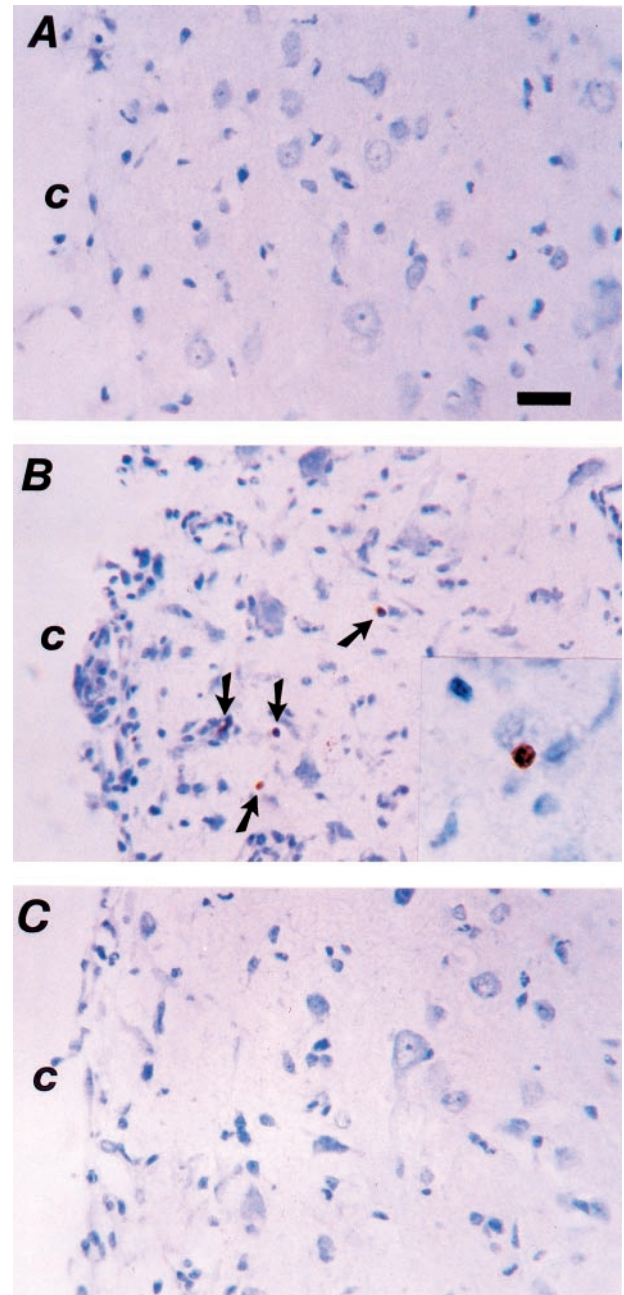


Figure 2 ISEL detection of apoptotic cells following TNF- α infusions and oral CPI-1189 treatment. Photomicrographs showing the neocortex adjacent to the cannula tract for representative Saline/Vehicle (A), TNF- α /Vehicle (B), and TNF- α /CPI-1189 (C) treated animals. Note the presence of apoptotic cells in the TNF- α /vehicle treated animal (arrows in B) and the lack of apoptotic cells in the same brain region of the other two treatment groups (A and C). Insert in (B) shows a single apoptotic cell at 1000 \times magnification. Bar in (A) is 25 μ m in length and indicates the magnification of all three photomicrographs. Abbreviations: c, cannula tract.

CPI-1189 decreased GFAP staining in the neocortex induced by 3 days of intracerebral infusions, as Sal/Veh treated animals had a significantly greater per cent of GFAP staining than TNF/Veh

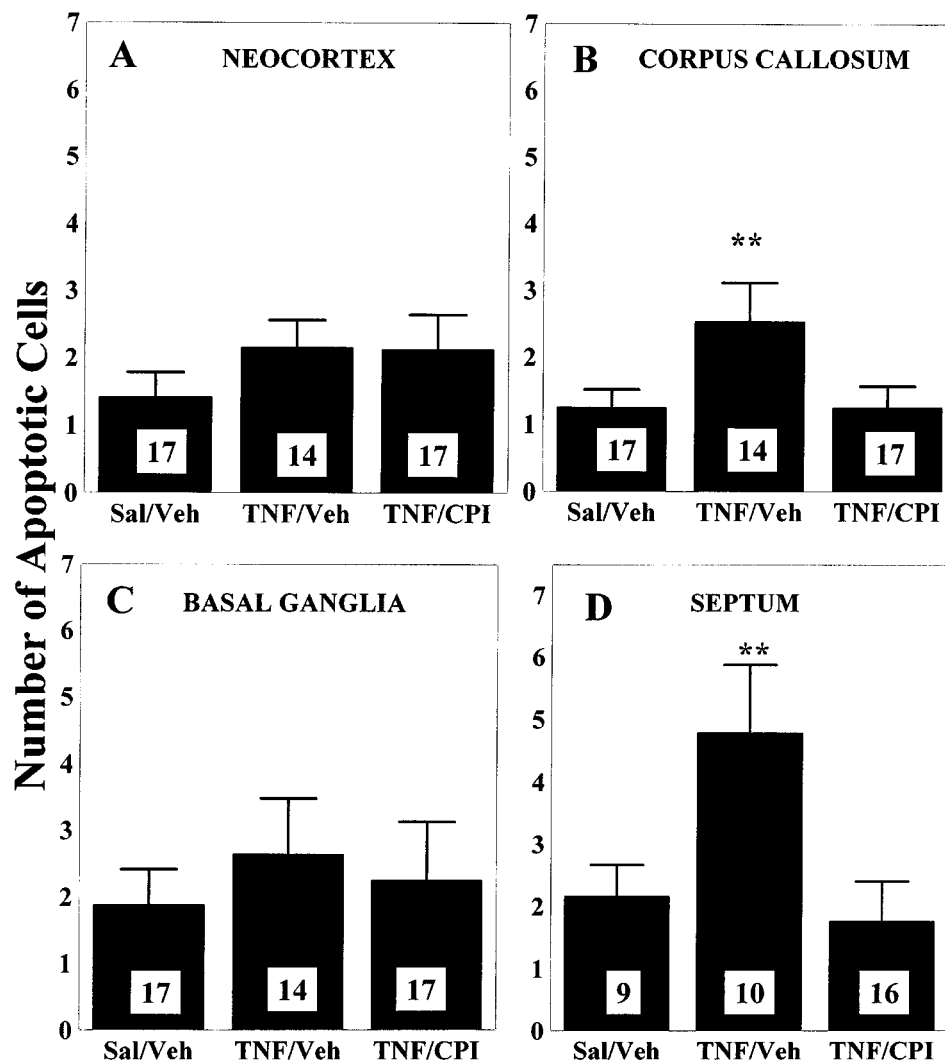


Figure 3 Effects of intracerebroventricular infusions of TNF- α and oral treatments of CPI-1189 on apoptosis in specific brain areas surrounding the i.c.v. infusion site. Data represent mean \pm s.e.m., and the number at the base of each bar indicates the number of infusion sites for that group. (A–D) The mean number of apoptotic cells in the neocortex (A), corpus callosum (B), basal ganglia (C), and septum (D). The abscissa indicates the i.c.v./oral treatment of the groups. **Indicates significantly greater than both Sal/Veh and TNF/CPI. Significance at $P \leq 0.05$.

treated animals ($P \leq 0.04$) or TNF/CPI treated animals ($P \leq 0.004$).

GFAP staining in the corpus callosum after 3 days of treatment with TNF- α alone produced no significant effect on the per cent GFAP staining (Figure 5B), as the TNF/Veh treated group was not significantly different from either Sal/Veh or TNF/CPI treated groups. Similar to GFAP staining in neocortex, however, the co-administration of CPI-1189 for 3 days decreased GFAP staining in the corpus callosum, since TNF/CPI treated animals had a significantly lower per cent of GFAP staining than Sal/Veh animals ($P \leq 0.008$). Figure 6 shows GFAP staining in the corpus callosum of a Sal/Veh treated animal (A) and a TNF/CPI treated animal (B). Note the decreased incident and density of staining in the animal treated with CPI compared to

the control animal. In the basal ganglia, TNF/Veh treated animals again were not significantly different from TNF/CPI or Sal/Veh treated animals (Figure 5C). However, as was the case for both the neocortex and corpus callosum, TNF/CPI treated animals had a significantly lower per cent of GFAP staining in the basal ganglia than the Sal/Veh treated group ($P \leq 0.02$). In the septum (Figure 5D), there were no significant differences in the per cent of GFAP staining.

IgG analysis

Analysis of the total density of IgG staining was done by averaging the density of IgG staining from both areas of the corpus callosum and the anterior commissure. No significant difference in IgG staining was found in total density of IgG staining, suggest-

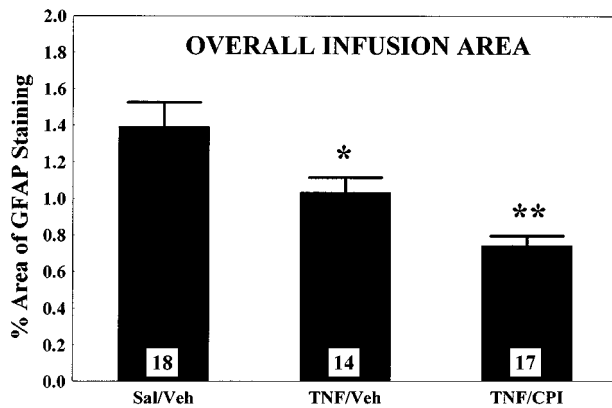


Figure 4 Average per cent area of glial fibrillary acidic protein staining around the overall infusion area after TNF- α infusions and/or oral CPI-1189 treatment for 3 days. The overall per cent area of glial fibrillary acidic protein staining was averaged across the neocortex, corpus callosum, and basal ganglia. Data represent mean \pm s.e.mean, and the number at the base of each bar indicates the number of infusion sites for that group. The abscissa indicates the i.c.v./oral treatment of the groups. *Indicates significantly less than Sal/Veh. **Indicates significantly less than both Sal/Veh and TNF/Veh. Significance at $P \leq 0.05$.

ing that neither TNF- α and CPI-1189 grossly affected the blood-brain barrier (Figure 7A). Looking specifically at IgG staining in the corpus callosum at the level of the infusion site, there was no significant difference between TNF/Veh and Sal/Veh treated animals at (Figure 7B). However, TNF- α infusions combined with CPI-1189, produced a significant decrease in IgG staining after 3 days of treatment compared to either Sal/Veh or TNF/Veh treatments ($P \leq 0.009$ and 0.02 respectively). Thus treatment with CPI-1189 effected blood-brain barrier integrity near the infusion site by providing an enhanced blood-brain barrier effect when given for 3 days.

At the caudal site of the corpus callosum, an area away from the site of direct ICV infusions, no significant differences were found between the groups after 3 days of treatment (Figure 7C). Also, as shown in Figure 7D, there were no significant differences in IgG staining in the anterior commissure between groups. This indicates that, at a site divorced from mechanical damage but at the coronal level of infusion, there was no effect of TNF- α or CPI-1189 on blood-brain barrier integrity.

Neurochemistry

Analysis of lipid peroxidation via TBAR formation indicated no significant differences between the groups after 3 days of treatment (Figure 8A). Neither treatment with TNF- α or CPI-1189 appeared to induce changes in lipid peroxidative damage as measured by this assay. As was the case for lipid peroxidation, hydroxyl free radical formation (via hydroxylation of salicylate into DHBA) was not

significantly different between the groups treated for 3 days (Figure 8B).

Discussion

The present study first demonstrates that multiple intracerebral infusions of the inflammatory cytokine TNF- α induce apoptosis within selective brain areas around the infusion site and that co-administration of the novel compound CPI-1189 prevents this TNF- α induced apoptosis. Co-treatment of CPI-1189 in the TNF- α model also suppressed GFAP staining in all areas except the septum. Blood-brain barrier integrity was not affected by TNF- α infusions, but concurrent oral treatment with CPI-1189 appeared to provide an enhanced blood-brain barrier selectively at the infusion site. Lastly, no effect of TNF- α or concurrent CPI-1189 treatment was found on two measures of oxidative stress, suggesting that classical oxidative mechanisms may not be the prominent agent in TNF- α induced apoptosis. In addition, CPI-1189 may be exerting at least some of its protective actions through mechanisms not immediately associated with decreasing concentrations of superoxide anion and hydroxy radicals.

We have previously reported that long-term intracerebral TNF- α infusions induce cognitive deficits, weight loss, and ventricular enlargement (Bjugstad *et al*, 1998) – all of which characterize ADC. Moreover, we further reported that co-administration of CPI-1189 prevented all of these effects induced by TNF- α (Bjugstad *et al*, 1998). The results of the present study extend our characterization of the TNF- α infusion model and the effects of CPI-1189 therein by investigating effects of TNF- α and CPI-1189 on cellular, cerebrovascular, and oxidative measures relevant to ADC. Cellularly, TNF- α induced apoptosis independent of hydroxy-radical formation and the induced apoptosis was prevented by CPI-1189. Moreover, our results suggest that CPI-1189 can attenuate GFAP/astrogliosis.

Neurons, glia, and endothelial cells have all been found undergoing apoptosis in the brains of AIDS patients, with many such cells found in the neocortex and basal ganglia (An *et al*, 1996; Petito *et al*, 1995, Shi *et al*, 1996). Similar to our earlier study (Bjugstad *et al*, 1998), we currently show that ICV infusions of TNF- α induced an overall elevation in apoptosis surrounding the infusion site that was over and above the apoptosis induced mechanically by saline (control) infusions. Additionally, we now report that significant TNF- α -induced apoptosis occurred in some, but not all brain regions bordering the TNF- α infusion site (i.e. septum and corpus callosum). This is not unusual, as different brain regions show different susceptibilities to cell damage (i.e. lipid and protein oxidation) and distinct methods of apoptosis regulation (Sack *et al*, 1996; Dubey *et al*, 1995; Bernier and Parent,

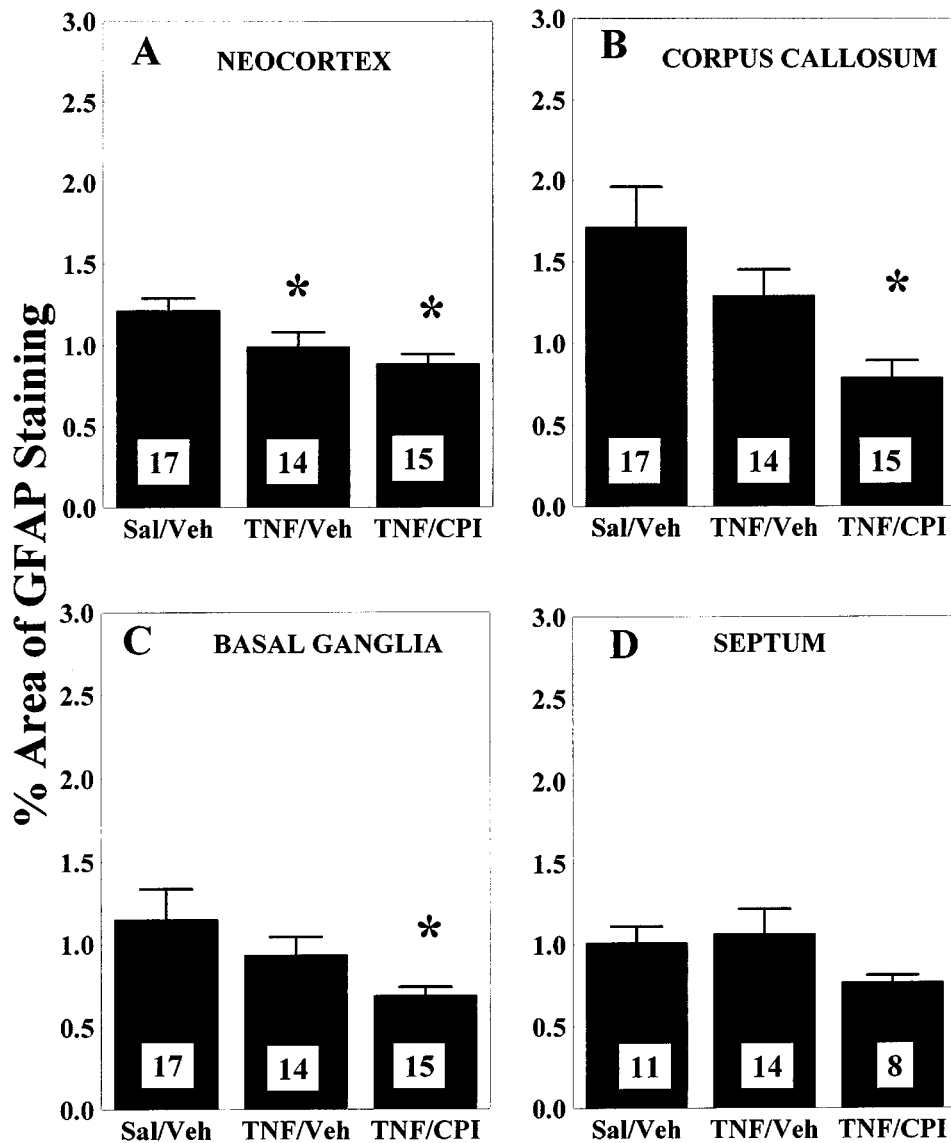


Figure 5 The effect of intracerebroventricular TNF- α infusions and oral CPI-1189 on per cent of glial fibrillary acidic protein staining in neocortex (A), corpus callosum (B), basal ganglia (C), and septum (D). Data represent mean \pm s.e.m. per cent area of glial fibrillary acidic protein stain, and the number at the base of each bar indicates the number of infusion sites for that group. The abscissa indicates the i.c.v./oral treatment of the groups. *Indicates significantly less than the Sal/Veh treated group. Significance at $P \leq 0.05$.

1998). The apoptotic cells seen in the corpus callosum are most likely oligodendrocytes. Thus, the present study provides *in vivo* evidence for a link between TNF- α and cytotoxicity in oligodendrocytes (Wilt *et al*, 1995; Selmaj *et al*, 1991a; Probert *et al*, 1997). Co-administration of CPI-1189 eliminated not only the overall increase in apoptosis induced by TNF- α , but also the regionally increased apoptosis in septum and corpus callosum induced by TNF- α . These results suggest that CPI-1189, or similar compounds, may be able to reduce the increased apoptosis that is seen in HIV-1 individuals having CNS involvement (An *et al*, 1996; Dickson *et al*, 1995; Petit *et al*, 1995; Masliah *et al*, 1992).

While TNF- α positive cells can be found in close proximity to GFAP positive cells in AIDS brains, few studies (all of which were *in vitro*) have actually looked at the direct effects of TNF- α on GFAP expression in astrocytes (Seilhean *et al*, 1997). Proliferation of astrocytes can occur after exposure to TNF- α (Barna *et al*, 1990; Selmaj *et al*, 1990), and cell identity has often been verified using GFAP immunohistochemistry. However, TNF- α may or may not stimulate the expression of GFAP. Depending on whether human or murine TNF is involved, GFAP mRNA and protein can be down-regulated (Murphy *et al*, 1995; Oh *et al*, 1993; Selmaj *et al*, 1991b). A down-regulation of GFAP was seen using 'human' recombinant TNF- α in either bovine or

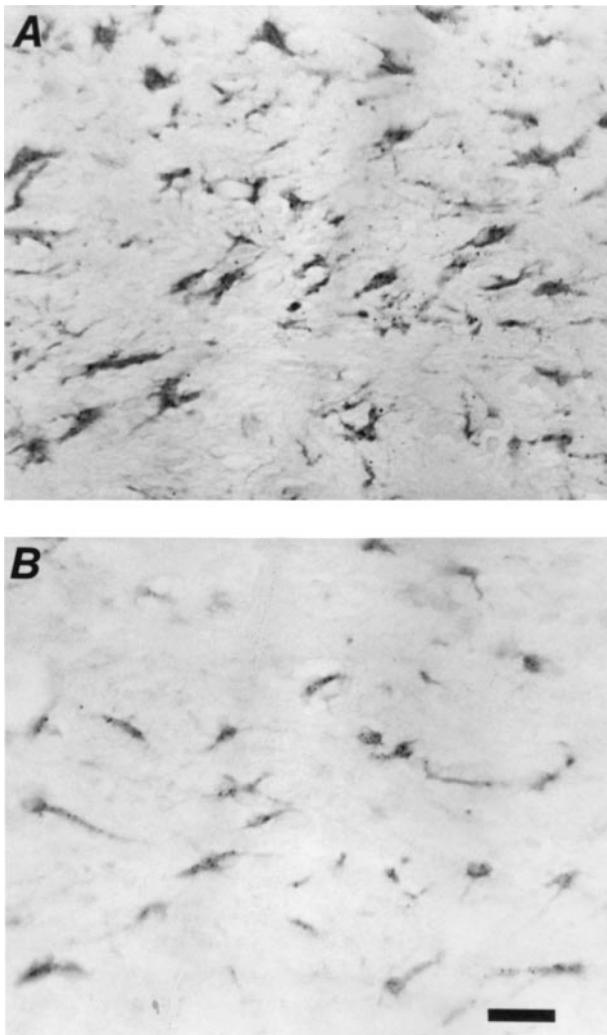


Figure 6 Effects of TNF/CPI treatment on glial fibrillary acidic protein immunohistochemical staining. Photomicrographs are from the corpus callosum of a representative Saline/Vehicle treated animal (A) and a TNF/CPI treated animal (B). Note the greater number and staining intensity of astrocytes in Sal/Veh treated animal (A) compared to the TNF/CPI treated animal (B). Bar in (B) is 25 μ m in length and indicates the magnification of both photomicrographs.

murine astrocyte cultures (Oh *et al*, 1993; Selmaj *et al*, 1991b). In the present study, we used 'human' recombinant TNF- α in our rat ICV infusion model. This may explain why we found no increase, but an occasional decrease, in GFAP staining in our TNF- α treated groups.

While TNF- α infusions alone, reduced astrogliosis in only one area specifically, there was a more wide-spread and a more enhanced effect of CPI-1189 co-administration on astrogliosis (Seilhean *et al*, 1997). In the overall area surrounding the infusion site, CPI-1189 further reduced GFAP staining compared to TNF- α alone, suggesting a better suppression of astrogliosis formation. This effect of CPI-1189 was also found within specific

brain areas around the infusion site. In the neocortex, basal ganglia, and corpus callosum, CPI-1189 significantly decreased the per cent of GFAP staining. Thus, CPI-1189 seems to suppress the astrogliotic response to repeated intracerebral infusions. Our results are in accord with another study in which the antioxidant, LY231617, decreased the induction of GFAP RNA in an ischemic model (May *et al*, 1996). During a 30 min four vessel occlusion, increased RNA levels of GFAP are normally found in the hippocampus and caudate. However treatment with LY231617 decreased GFAP RNA in both areas. Our combined studies suggest a role for antioxidants in suppressing or delaying the formation of astrogliosis in neurodegenerative conditions.

Several studies have found that AIDS patients show signs of blood-brain barrier disruption (Petito and Cash, 1992; Rhodes, 1991; Resnick *et al*, 1985). In the present study, we found extensive IgG staining (i.e. reduced blood-brain barrier integrity) restricted primarily in white matter areas near the cannula tract. While some increase in IgG staining was expected due to cannulation-induced damage, we saw no additional increase in IgG staining as a result of TNF- α treatment. Co-administration of CPI-1189 for 3 days did, however, decrease IgG staining (i.e. increase blood-brain barrier integrity) at the site most effected by cannula damage. It is important to note, however, that this effect of CPI-1189 co-administration was observed only near the cannula infusion site. CPI-1189 did not affect IgG staining at sites divorced from the cannula tract, suggesting that treatment with CPI-1189 alone in uncannulated animals would not appreciably affect the blood-brain barrier. The fact that no increase in IgG staining was seen in groups treated with TNF- α alone may be explained by the cannula tracts themselves. Any effect of TNF- α (or CPI-1189) would have to overcome the extensive IgG staining produced locally by the cannulation itself. Thus, any subtle, localized effects of TNF- α treatment could have been obscured by this mechanical damage.

We had anticipated some effect of intracerebral TNF- α infusions on measures of oxidative stress since multiple studies have shown that TNF- α can induce production of reactive oxygen species, which can be part of the process by which TNF- α induces apoptosis (Shoji *et al*, 1995; Greenspan and Aruoma, 1994; Meda *et al*, 1995 and Goosens *et al*, 1995). In addition, treatment with antioxidants has been reported to prevent TNF- α induced apoptosis (Goosens *et al*, 1995; Shoji *et al*, 1995). Although all of the aforementioned were *in vitro* studies, our own *in vivo* studies have shown that CPI-1189, a compound structurally similar to the antioxidant PBN, not only prevents TNF- α induced apoptosis, but also prevents TNF- α induced cognitive impairment, weight loss, and ventricular enlargement

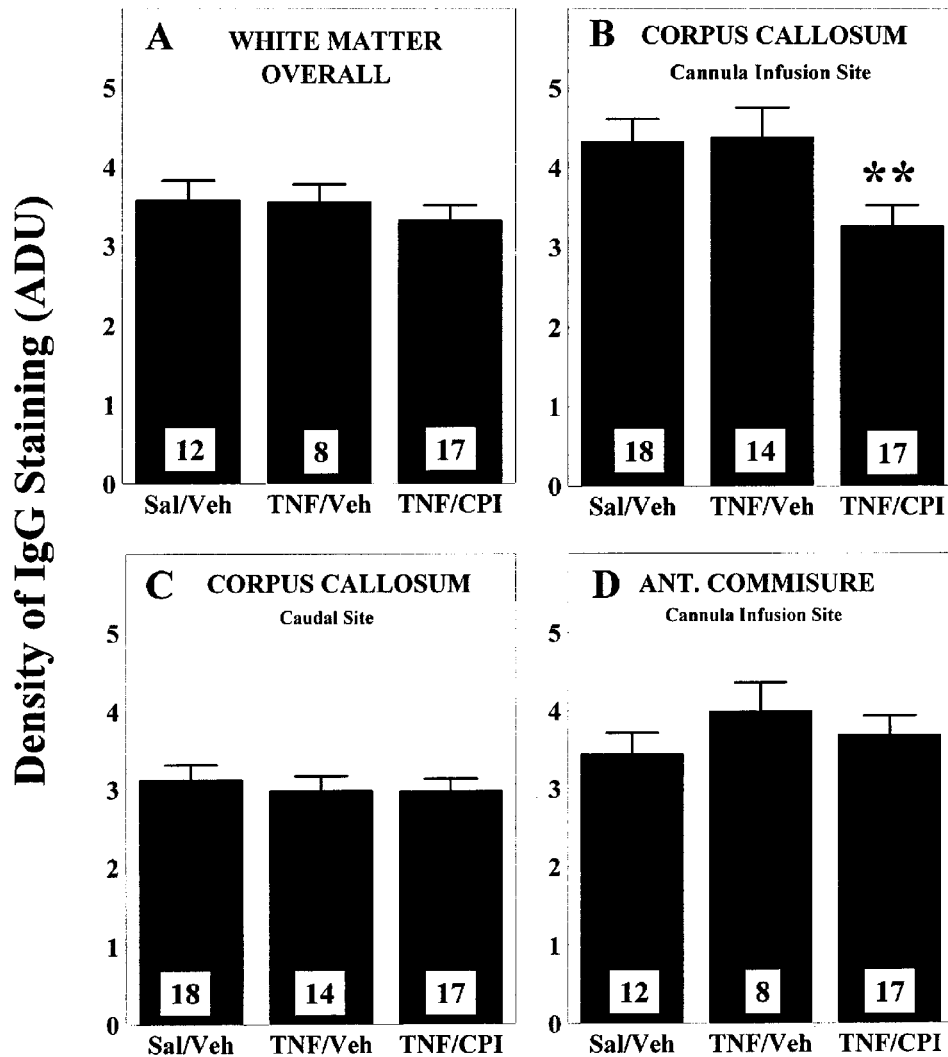


Figure 7 The effects of intracerebroventricular infusions of TNF- α and oral treatment with CPI-1189 on the density of IgG staining in subcortical and deep white matter. Density values represent a mean \pm s.e.m. taken from two $200 \times 250 \mu\text{m}$ images per side, and the number at the base of each bar indicates the number of infusion sites for that group. The abscissa indicates the i.c.v./oral treatment of the groups. (A) Average density of IgG staining in white matter. The density of IgG staining was averaged from values obtained from both corpus callosum areas and the anterior commissure. (B) The density of IgG staining in the corpus callosum near the cannula tract. (C) The density of IgG staining in the corpus callosum at a caudal site away from the cannula tract. (D) The density of IgG staining in the anterior commissure. **Indicates significant less than the Sal/Veh and TNF/Veh treated groups. Significance at $P \leq 0.05$. Abbreviations: ADU, arbitrary density units.

(Bjugstad *et al*, 1998). There are several possible explanations for TNF- α 's inability to affect measures of oxidative stress (i.e. lipid peroxidation and hydroxyl radical formation) in the present *in vivo* study. First, TNF- α effects on measures of oxidative stress may have occurred more immediately following TNF- α infusion than the 3–5 h post-infusion time point selected for euthanasia. Second, the block of brain tissue dissected out from around the cannula infusion site may have been too large for detecting neurochemical changes close to the ventricular wall, thus masking any such changes. Third, measures of oxidative stress other than those selected may be more profoundly affected by TNF- α

infusions. Fourth, recent experimental evidence suggests that CPI-1189 exerts its therapeutic effects through attenuating key signal transduction pathways rather than by free radical trapping (Hensley *et al*, 2000).

The mechanism by which CPI-1189 accomplishes its protective effect is even less well understood than how TNF- α induces apoptosis. Because the TNF- α treatment did not increase TBARs or hydroxyl radicals but did induce apoptosis, which could be blocked by CPI-1189, suppressing production of reactive oxygen species may not be the major mechanism mediating the anti-apoptotic action of CPI-1189. However, our experiment could not

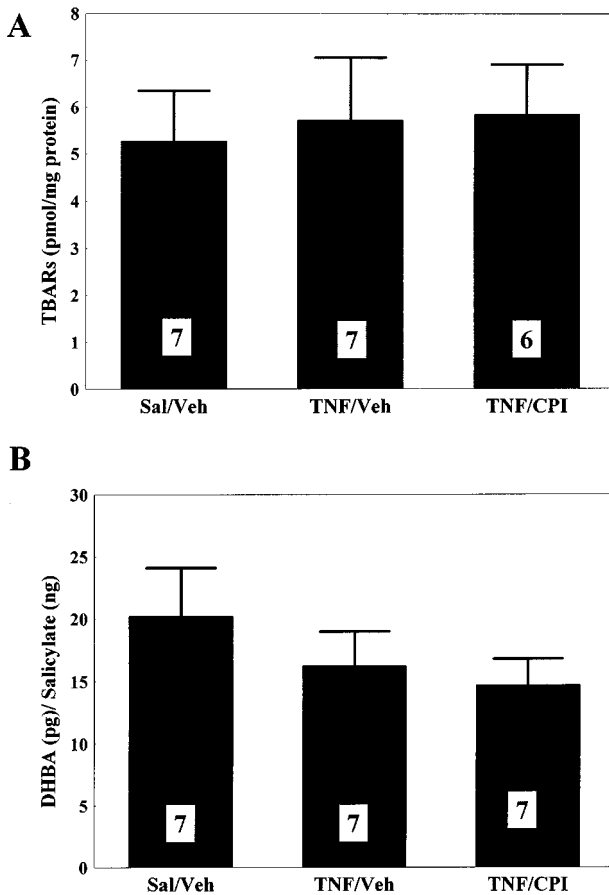


Figure 8 The effects of intracerebroventricular TNF- α infusions and oral CPI-1189 treatment on oxidative stress in brain tissue surrounding the cannula site. **(A)** Lipid peroxidation, as indexed by the formation of thiobarbituric acid reactive products (TBARs), in brain tissue around the infusion site from animals in each of the three treatment groups. **(B)** Hydroxyl free radical production, as indexed by the hydroxylation of salicylate to 2,5 dihydroxybenzoic acid, in brain tissue around the infusion site from animals in each of the three treatment groups. Data represents the mean \pm s.e. mean and the number at the base of each bar indicates the number of infusion sites for that group.

exclude the possibility that CPI-1189 suppresses the production early after the TNF- α treatment of small amounts of reactive oxygen species, which may be enough to induce apoptosis. It should be noted that CPI-1189 does not interfere with the binding of TNF- α to either its p55 or p75 binding sites (unpublished observations, Centaur Pharmaceuticals, Inc.). CPI-1189 more likely acts in the signal transduction pathway activated by the binding of TNF- α to its p55 binding site. In several experiments, CPI-1189 was found not to affect levels of NF- κ B, but did prevent the decrease of bcl-2 (an endogenous anti-oxidant and anti-apoptotic agent) induced by TNF- α (unpublished observations, Centaur Pharmaceuticals, Inc.). Current studies are focused on characterizing how CPI-1189 prevents this loss of bcl-2, and establishing the extent that

maintenance of bcl-2 levels is responsible for the anti-apoptotic effect shown by CPI-1189 in numerous *in vitro* and *in vivo* experiments (unpublished observations, Centaur Pharmaceuticals, Inc.).

To summarize the results of this study, we have presented a novel rodent model for ADC based on CNS inflammation induced through intracerebral infusions of TNF- α . We have previously shown that this model exhibits cognitive deficits, weight loss, and gross pathological changes similar to those seen in ADC (Bjugstad *et al.*, 1998). In the present study, we extended our investigations of this model to include cellular/neurochemical changes present in ADC – specifically, apoptosis, astrogliosis, disruption of the blood-brain barrier, and measures of oxidative stress. We found that ICV infusions of TNF- α induced overall and regionally specific increases in apoptosis. In addition, co-administration of CPI-1189 prevented the cell loss induced by TNF- α infusions. Both TNF- α and CPI-1189 appeared to inhibit GFAP staining, although CPI-1189 appears to have a more potent effect than TNF- α . The relatively negative results of TNF- α infusions on IgG staining and oxidative stress in no way compromise the validity of our model as a viable model of CNS inflammation for ADC. The most salient characteristics of ADC (i.e. the dementia, weight loss, ventricular enlargement, and apoptosis) can be induced by ICV infusions of TNF- α and, more importantly, they can be prevented through the administration of CPI-1189. It is in that context that clinical trials are currently underway to determine the efficacy of CPI-1189 in treating/preventing ADC.

Materials and methods

General

Young adult (2–3 months old; 275–300 g) Sprague-Dawley male rats had stainless steel cannulas permanently implanted into both lateral ventricles, as described in our preceding study (Bjugstad *et al.*, 1998). Animals were given free access to food/water and were kept on a 12 h light/dark schedule during the course of the study. Beginning 4–5 days after the intracerebral ventricular (i.c.v.) surgery, animals were intraventricularly infused bilaterally with either human recombinant TNF- α (50 ng in a 1 μ l infusion, which is 2.9 μ moles/ μ l; Calbiochem-Novabiochem, Co.) or isotonic saline vehicle once daily for 3 days. During this period, animals also received concurrent twice daily oral treatment with either CPI-1189 (20 mg/kg, which is 8.5 pmoles/kg; Centaur Pharmaceuticals, Inc.) or methyl-cellulose vehicle (1 ml/kg). On the last day, 3–5 h after i.c.v. oral treatments were given, animals were killed and brains were removed. These animals had brain tissue prepared for immunohistochemical analysis of apoptosis, astrogliosis (GFAP staining), and blood-brain barrier integrity (IgG staining). Because

i.c.v. surgery/infusions can cause damage affecting immunohistochemical measures, analyses are presented in terms of increased/decreased apoptosis, GFAP staining, and/or IgG staining beyond that which is induced by surgery/infusion seen in the Saline/Vehicle control animals. Parenthetically, use of the contralateral 'uninfused' side of unilaterally infused animals could not be done to avoid cannula damage because of minimal infusate transfer to the uninfused ventricle. A second set of animals, undergoing identical 3 day i.c.v. iral treatment procedures, had their brain tissue prepared for neurochemical analysis of lipid peroxidation via TBAR assay and hydroxyl radical formation via salicylate hydroxylation. Throughout the text, each group of animals will be referred to in abbreviated form according to their i.c.v. oral treatments (i.e. Sal/Veh, TNF- α /Veh, or TNF- α /CPI). There were 9, 7 and 9 animals in the Veh/Sal, TNF/Sal and TNF/CPI treated groups respectively, which were used for neurohistology. For neurochemistry, there were 7 animals in each group.

Immunohistochemical analysis

On the last day of treatment, animals were anesthetized with sodium pentobarbital (50 mg/kg), 3–5 h after the last i.c.v. infusion and intracardially perfused with 4% neutral buffered formalin. The brains were removed and stored overnight in formalin. A 3 mm thick coronal slice was then taken at the cannula site and paraffin embedded, keeping the melted paraffin below 60°C to avoid the occurrence of false positives during apoptosis staining. From the slice containing the cannula site, 6 μ m sections were collected at the deepest point of cannula penetration. A 3 mm slice was also embedded and sectioned from the dorsal hippocampal area for IgG staining. All cannula tip locations were determined and only those animals having at least one side with the cannula tip clearly located within the lateral ventricle were used in this study. Occasionally, an animal's cannula was placed caudal enough such that the septum could not be used. Because of this, the number of determinations for septal measures is lower than for other areas. As such, analyses which involved an overall evaluation (i.e. total number of apoptotic cells and overall GFAP staining) did not include the septum. Immunohistochemical analyses were performed with the mean of two brain sections. Left and right sides were considered independent determinations to allow any animal with at least one cannula in the correct location to be included in analyses.

Apoptosis staining

Detection of apoptotic cell bodies was done using NeuroTACS, an *in situ* end-labeling kit (Trevigen, Inc.). All reagents, unless otherwise noted, were

provided in the NeuroTACS kit. Tissue samples were deparaffinized and incubated with Neuropore (a permeabilization and blocking reagent) for 4 h at room temperature. Samples were washed for 2 min in phosphate buffered saline (PBS) and placed in 3% hydrogen peroxide/methanol solution for 5 min. Samples were then placed into two baths of Klenow labeling buffer for 2 min each. The labeling reaction (5 n μ l of 10 \times labeling buffer, 45 n μ l of distilled water, 1 n μ l of Klenow dNTP, and 1 n μ l Klenow polymerase; n =number of sections used) was then placed onto each section and incubated at 37°C for 1 h in a humidified chamber. Sections were then transferred to Klenow stop buffer for 5 min and washed twice in PBS for 2 min. Streptavidin labeling solution (100 μ l PBS and 1 μ l Strep-HRP) was applied to each section and incubated at room temperature for 15 min. Samples were washed in PBS and placed in a DAB solution (50 ml PBS, 250 μ l DAB, 50 μ l 30% hydrogen peroxide) for 8 min followed by two rinses in distilled water. Samples were then counterstained with a hematoxylin blue dye, dehydrated, and coverslipped.

Two brain sections were processed from each animal and results were averaged together. Quantification of parenchymal apoptotic cells around the i.c.v. infusion and located in the neocortex, corpus callosum, basal ganglia, and septum was done for each infusion site using a Zeiss Universal light microscope. Under 100 \times magnification, the number of apoptotic cells within 1–1.5 mm of the cannula tract/ventricular lining was counted for each area. Extreme values in each group (greater than three standard deviations away from the group mean) were not included in statistical analysis. In addition, a total number of apoptotic cells was calculated from the combined numbers found in the neocortex, corpus callosum, and basal ganglia. All data was analyzed using one-way ANOVAs with *post hoc* Fisher LSD ($P \leq 0.05$ significance) for treatment groups.

GFAP staining

Brain sections were deparaffinized and incubated for 1 h at room temperature with a 1 : 400 dilution of mouse monoclonal anti-GFAP IgG (Accurate Chemical and Scientific Corp.) in Neuropore (Trevigen, Inc.). Sections were then washed in 100 mM Tris-HCl buffer and incubated for 30 min at room temperature with a 1 : 20 dilution of anti-mouse IgG (Kirkegaard and Perry Lab, Inc.) in Neuropore. Sections were again washed with 100 mM Tris-HCl buffer. Color development was done using a red label azo-dye solution provided in the NeuroTACS apoptosis kit (Trevigen, Inc.). Samples were incubated with the red label solution for 10 min in the dark at room temperature. The reaction was stopped by washing the section three times in distilled water for 2 min and then coverslipped.

The degree of astrogliosis was quantified by measuring the per cent of GFAP staining present in a digital image. Quantification of GFAP staining around each infusion site (in the neocortex, corpus callosum, basal ganglia, and septum) was done using digital images from two brain sections per animal and then averaged together. Digital computer images were taken through a light microscope using Snappy video snapshot software (Play, Inc.). Digital images were then analyzed for the area of glial fibrillary acidic protein staining from total area of the image using UTHSCSA/NIH Image Tool 1.25. At 100 \times magnification, two adjacent images in the basal ganglia and in the septum were taken along the ventricular wall of both hemispheres and from both brain sections (a total of four 500 \times 400 μ m images per side). Also at 100 \times magnification, eight images of neocortex were analyzed per hemisphere (two adjacent images on both sides of the cannula tract from both brain sections). The corpus callosum was analyzed at 200 \times magnification, with a single image (250 \times 200 μ m) taken on either side of the cannula tract producing two fields per hemisphere per brain section. All data was analyzed using one-way ANOVAs with *post hoc* Fisher LSD ($P \leq 0.05$ significance).

IgG staining

Biostain Super ABC mouse/rat IgG kit was used for IgG staining of brain sections at the infusion site, as well as brain sections taken at the dorsal hippocampal level. The IgG kit and all reagents were provided by Biomed, Inc. unless otherwise indicated. Sections were deparaffinized and placed in 1 \times automation buffer for 3 min. They were then placed in 1% hydrogen peroxide for 7 min and rinsed in automation buffer for 5 min. All subsequent steps were done in a humidified chamber at 37 $^{\circ}$ C unless otherwise indicated. Sections were then incubated with a protein blocker for 10 min and rinsed in automation buffer for 5 min. After rinsing, the sections were incubated with anti-mouse/rat IgG antibody for 30 min and again washed with automation buffer. Sections were incubated with detector reagent for 60 min, cleared in distilled water, and incubated for 25 min with Vega red solution (Alkaline Phosphatase Chromogen Kit) for color development. After clearing with distilled water, each section was covered with Crystal mount and dry baked at 70 $^{\circ}$ C for 20 min.

General analysis of IgG staining revealed a specific pattern of staining which was seen in all three groups – Sal/Veh, TNF/Veh, and TNF/CPI. The brain areas (i.e. neocortex, corpus callosum, basal ganglia, and septum) directly adjacent to the cannula site were intensely stained due to cannula insertion. In areas somewhat divorced from the site of cannulation, the white matter (i.e. corpus callosum, anterior commissure, and striations in the basal ganglia) showed relatively dark IgG

staining. IgG staining in areas of grey matter (neocortex, basal ganglia, and septum) that were not directly near the cannula site, showed very light staining. Because of the light staining in these grey matter areas, the density of staining could not be captured with our image analysis system, thus quantitative analysis for group differences was done using areas of white matter.

For IgG quantitative analysis, the density of stain was evaluated in: (1) the corpus callosum at the site of the cannula tract; (2) the corpus callosum at the level of the dorsal hippocampus, and (3) the anterior commissure. The caudal corpus callosum site was used to evaluate the extent of possible blood-brain barrier disruption away from the infusion site, while the anterior commissure was chosen as a control area which would not have been directly affected by mechanical damage from the cannula and ICV infusions. Quantification of IgG staining was done by analyzing the density of stain (arbitrary density units – ADU). Digital computer images (250 \times 200 μ m) were taken through a light microscope at 200 \times magnification using Snappy video snapshot software (Play, Inc.). Images for both the rostral and caudal corpus callosum sites were taken along the neocortical concavity. Computer images were then analyzed for the mean density of IgG staining within the area of the image using UTHSCSA/NIH Image Tool 1.25. All data was analyzed using one-way ANOVAs with *post hoc* Fisher LSD ($P \leq 0.05$ significance) for treatment groups.

Neurochemical analyses

On the last day of ICV/oral treatment, the second group of animals was injected i.p. with salicylic acid, sodium salt (100 mg/kg=0.63 mmole/kg in isotonic saline, Aldrich Chemical Co., Inc.) 30 min prior to decapitation for the purposes of salicylate hydroxylation described below. After decapitation, the brain was removed and a 3 \times 3 mm cube of tissue surrounding the cannula tract was dissected out from each side of the brain. Each tissue cube contained neocortical, basal ganglia, and septal tissue, as well as corpus callosum. Samples were quick frozen on dry ice and stored at –80 $^{\circ}$ C until neurochemical analyses could be done. The left cannula tract tissue samples were used for TBAR analysis and samples from the right side were used for salicylate hydroxylation.

TBAR assay

Analysis of lipid peroxidation by thiobarbituric acid reactive product (TBAR) formation followed our basic methodology (Sengstock *et al*, 1997). A 10% tissue homogenate was made by sonicating tissue samples in isotonic saline in isotonic saline to which desferrioxamine (0.2 μ g/ μ l) was added to chelate the increased free iron resulting from tissue sonication. A 10 μ l sample was withdrawn for

protein determination using the BCA method (Pierce Chemical, Co.). A sample of 200 μ l was withdrawn from the remaining homogenate and added to 300 μ l of 25% trichloroacetic acid (in distilled water), 150 μ l of 1% thiobarbituric acid (in distilled water) and 10 μ l of butylated hydroxytoluene (in 100% ethanol). Butylated hydroxytoluene was used as a secondary antioxidant to desferrioxamine. Sample solutions were then vortexed and incubated in a dry bath at 90°C for 45 min. Samples were cooled to room temperature, centrifuged (15 000 \times g for 10 min), and absorbance of the supernatant was spectrophotometrically determined at 535 nm using a Hewlett Packard 8450A diode array spectrophotometer. The concentration of TBAR products was calculated using a standard curve of 1,1,3,3-tetramethoxypropane (concentrations ranging from 0 to 20 pmol/ μ l) with values expressed as pmol TBAR/ μ g protein. All data was analyzed using one-way ANOVAs with *post hoc* Fisher LSD ($P \leq 0.05$ significance) for 3-day treated groups.

Salicylate hydroxylation

To evaluate hydroxyl free radical formation around the cannula infusion site, the oxidation of salicylate was measured. In the presence of hydroxyl free radicals, salicylate forms dihydroxybenzoic acid by-products (McCabe *et al*, 1997). The procedure for salicylate hydroxylation was based on the primary methodologies of McCabe *et al* (1997) and Sloot and Gramsbergen (1995). As stated previously, animals were injected i.p. with 100 mg/kg salicylic acid 30 min prior to sacrifice via decapitation. Following brain removal from the cranium, a 3 \times 3 mm block of brain tissue surrounding the cannula tract was dissected out and processed for HPLC detection of salicylate and 2,5-dihydroxybenzoic acid (DHBA). Tissues were sonicated to form a 10% homogenate

in monochloroacetic acid mobile phase (0.15 M chloroacetic acid, 0.05 mM sodium octyl sulfate, 1 mM disodium EDTA, and pH to 2.9 with sodium hydroxide and 4% v/v acetonitrile). Homogenates were centrifuged (12 000 \times g for 5 min). The supernatant was removed and passed through a 0.2 μ m cellulose acetate Microspin centrifuge filter. Samples were then kept on ice until injected into the HPLC system. Stock solutions of salicylic acid and 2,5 DHBA (Aldrich Chemical Co., Inc.) for standard curves were also made with monochloroacetic acid mobile phase in concentrations ranging from 5–50 ng salicylate/10 μ l and 5–400 pg DHBA/10 μ l.

An HPLC system was used to measure the concentrations of salicylate and DHBA in the standards and brain tissue samples. A reverse-phase C18 Microsorb-MV column (3 μ m, 4.6 \times 100 mm; Microsorb, Rainin) was used to separate analytes. Salicylate was detected using a UV-absorbance detector with a 278 nm filter (Spectrasorb-UV). A BAS LC-4C electrochemical detector (Bioanalytical Systems), placed after the UV detector, was set at an oxidation potential of 250 mV against an Ag/AgCl reference electrode at 2 nA. The mobile phase, as described above, was passed through the system at 1 ml/min at 1.63 kpsi. Sample volume was 10 μ l. Peak area was measured using Rainin Analytic software package and was used to determine the amount of salicylate and DHBA in brain tissue samples. Data was analyzed as a ratio of DHBA to salicylate (pg/ng). All data was analyzed using one-way ANOVAs with *post hoc* Fisher LSD ($P \leq 0.05$ significance) for 3-day treated groups.

Acknowledgements

The authors would like to thank John Soto for excellent animal care.

References

- An SF, Gionetto B, Scaravilli T, Tavolato B, Gray F, Scaravilli F (1996). Programmed cell death in brains of HIV-1 positive AIDS and pre-AIDS patients. *Acta Neuropathol* **91**: 169–173.
- Artigas J, Grosse G, Miedobitek F, Kassner M, Risch W, Heise W (1994). Severe toxoplasmic ventriculomeningoencephalomyelitis in two AIDS patients following treatment of cerebral toxoplasmic granuloma. *Clin Neuropathol* **13**: 120–126.
- Aylward EH, Brettschneider PD, McArthur JC, Harris GJ, Schlaepfer TE, Henderer JD, Barta PE, Tien AY, Pearlson GD (1995). Magnetic resonance imaging measurement of gray matter volume reductions in HIV dementia. *Am J Psychiatry* **152**: 987–994.
- Aylward EH, Henderer JD, McArthur JC, Brettschneider PD, Harris GJ, Barta PE, Pearlson GD (1993). Reduced basal ganglia volume in HIV-1-associated dementia: Results from a quantitative neuroimaging. *Neurology* **43**: 2099–2104.
- Barna BP, Estes ML, Jacobs BS, Hudson S, Ransohoff RM (1999). Human astrocytes proliferate in response to tumor necrosis factor alpha. *J Neuroimmunol* **30**: 239–243.
- Bernier PJ, Parent A (1998). The anti-apoptosis bcl-2 proto-oncogene is preferentially expressed in limbic structure of the primate brain. *Neurosci* **82**: 635–640.
- Bjugstad KB, Flitter WD, Garland WA, Su GC, Arendash GW (1998). Preventative actions of a synthetic antioxidant in a novel animal model of AIDS dementia. *Brain Res* **795**: 349–357.
- Dal Pan GJ, McArthur JH, Aylward E, Selnes OA, Nance-Sproson TE, Kumar AJ, Mellits ED, McArthur JC (1992). Patterns of cerebral atrophy in HIV-1-infected individuals: Results of a quantitative MRI analysis. *Neuro* **42**: 2125–2130.
- Dickson DW (1995). Apoptosis in the brain: Physiology and pathology. *Am J Pathol* **146**: 1040–1044.

- Dubey A, Forster MJ, Sohal RS (1995). Effect of the spin-trapping compound N-tert-butyl- α -phenylnitron on protein oxidation and life span. *Arch Biochem Biophys* **324**: 249–254.
- Folks TM, Clouse KA, Justement J, Robson A, Duh E, Kehrl JH, Fauci AS (1989). Tumor necrosis factor α induces expression of human immunodeficiency virus in a chronically infected T-cell clone. *Proc Natl Acad Sci USA* **86**: 2365–2368.
- Gelman BB, Guinto Jr FC (1992). Morphometry, histopathology, and tomography of cerebral atrophy in the acquired immunodeficiency syndrome. *Ann Neurol* **32**: 31–40.
- Glass JD, Wesselingh SL, Selnes OA, McArthur JC (1993). Clinical-neuropathologic correlation in HIV-associated dementia. *Neurology* **43**: 2230–2237.
- Glass JD, Fedar H, Wesselingh SL, McArthur JC (1995). Immunocytochemical quantitation of human immunodeficiency virus in the brain: Correlations with dementia. *Ann Neurol* **38**: 755–762.
- Goosens V, Grooten J, DeVos K, Fiers W (1995). Direct evidence for tumor necrosis factor-induced mitochondrial reactive oxygen intermediates and their involvement in cytotoxicity. *Proc Natl Acad Sci USA* **92**: 8115–8119.
- Greenspan HC, Aruoma OI (1994). Oxidative stress and apoptosis in HIV infection: A role for plant derived metabolites with synergistic antioxidant activity. *Immunol Today* **15**: 209–213.
- Hensley K, Robinson KA, Pye QN, Floyd RA, Cheng I, Garland WA, Irwin I (2000). CPI-1189 inhibits interleukin 1 β -induced p39-mitogen activated protein kinase phosphorylation: an explanation for its neuroprotective properties. *Neurosci. Lett*, in press.
- Hestad K, McArthur HJ, Dal Pan GJ, Senes OA, Nance-Sproson TE, Aylward E, Mathews VP, McArthur JC (1993). Regional brain atrophy in HIV-1 infection: Association with specific neuropsychological test performance. *Acta Neurol Scand* **88**: 112–118.
- Jacobsen J, Gyldensted C, Brun B, Bruhn P, Helweg-Larsen S, Arlien-Soborg P (1989). Cerebral ventricular enlargement relates to neuropsychological measure in unselected AIDS patients. *Acta Neurol Scand* **79**: 59–62.
- Maruff P, Currie J, Malone V, McArthur-Jackson C, Mulhall B, Benson E (1994). Neuropsychological characterization of the AIDS dementia complex and rationalization of a test battery. *Arch Neurol* **51**: 689–695.
- Masliah E, Achim CL, Ge N, DeTeresa R, Terry RD, Wiley CA (1992). Spectrum of human immunodeficiency virus-associated neocortical damage. *Ann Neurol* **32**: 312–329.
- May PC, Clemens JA, Panetta JA, Smalstig EB, Stephenson D, Fuson KS (1996). *Brain Res Mol Brain Res* **42**: 145–148.
- McCabe DR, Maher TJ, Acworth IN (1997). Improved method for the estimation of hydroxyl free radical levels *in vivo* based on liquid chromatography with electrochemical detection. *J Chromatogr B* **691**: 23–32.
- Meda L, Cassatella MA, Szendrel GI, Otvos L, Baron P, Villalba M, Ferrari D, Rossi F (1995). Activation of microglial cells by β -amyloid protein and interferon- γ . *Nature* **374**: 647–650.
- Murphy GM, Lee YL, Jia XC, Yu ACH, Majewska A, Sony Y, Schmidt K, Eng LF (1995). TNF- α and basic fibroblast growth factor decrease glial fibrillary acidic protein and its encoding mRNA in astrocyte culture and glioblastoma cells. *J Neurochem* **65**: 2716–2724.
- Navia BA, Jordan BD, Price RW (1986a). The AIDS dementia complex: I. Clinical features. *Ann Neurol* **19**: 517–524.
- Navia BA, Cho ES, Petito CK, Price RW (1986b). The AIDS dementia complex: II. Neuropathology. *Ann Neurol* **19**: 517–524.
- Odeh M (1990). The role of tumor necrosis factor- α in acquired immunodeficiency syndrome. *J Int Med* **228**: 549–556.
- Oh YJ, Markelonis GJ, Oh TH (1993). Effects of interleukin-1 β and tumor necrosis factor- α on the expression of glial fibrillary acidic protein and transferrin in cultured astrocytes. *Glia* **8**: 77–86.
- Pace GW, Leaf CD (1995). The role of oxidative stress in HIV disease. *Free Radical Biol Med* **19**: 523–528.
- Peterson PK, Gekker G, Chao CC, Hu SX, Edelman C, Balfour HH, Verhoef J (1992). Human cytomegalovirus-stimulates peripheral blood mononuclear cells to induce HIV-1 replication via tumor necrosis factor- α -mediated mechanisms. *J Clin Invest* **89**: 574–580.
- Petito CK, Cash KS (1992). Blood-brain barrier abnormalities in acquired immunodeficiency syndrome: Immunohistochemical localization of serum proteins in post-mortem brain. *Ann Neurol* **32**: 658–666.
- Petito CK, Robert B (1995). Evidence of apoptotic cell death in HIV encephalitis. *Am J Pathol* **146**: 1121–1130.
- Power C, Kong PA, Crawford TO, Wesseling S, Glass JD, McArthur JC, Trapp BD (1993). Cerebral white matter changes in acquired immunodeficiency syndrome dementia: Alterations of the blood-brain barrier. *Ann Neurol* **34**: 339–350.
- Probert L, Akassoglou K, Kassiotis G, Pasparakis M, Alexopoulou L, Kollias G (1997). TNF- α transgenic and knockout models of CNS inflammation and degeneration. *J Neuroimmunol* **72**: 137–141.
- Resnick L, diMarzo-Veronese F, Schupback J, Tourtelotte WW, Ho DD, Muller F, Shapshak P, Vogt M, Groopman JE, Markham PD (1985). Intrablood-brain barrier syntheses of HTLV-III specific IgG in patients with neurologic symptoms associated with AIDS or AIDS-related complex. *New Engl J Med* **313**: 1498–1504.
- Rhodes RH (1991). Evidence of serum-protein leakage across the blood-brain barrier in the acquired immunodeficiency syndrome. *J Neuropathol Exp Neurol* **50**: 171–183.
- Sack CA, Socci DJ, Crandall BM, Arendash GW (1996). Antioxidant treatment with phenyl- α -tert-butyl nitron (PBN) improves the cognitive performance and survival of aging rats. *Neurosci Lett* **205**: 181–184.
- Seilhean D, Kobayashi K, He Y, Uchihara T, Rosenblum O, Katlama C, Bricaire F, Duychaerts C, Hauw JJ (1997). Tumor necrosis factor- α , microglia and astrocytes in AIDS dementia complex. *Acta Neuropathol* **93**: 508–517.
- Selmaj K, Raine CS, Farooq M, Norton WT, Brosnan CF (1991a). Cytokine cytotoxicity against oligodendrocytes: Apoptosis induced by lymphotoxin. *J Immunol* **147**: 1522–1529.

- Selmaj KW, Farooq M, Norton WT, Raine CS, Brosnan CF (1990). Proliferation of astrocytes *in vitro* in response to cytokines: A primary role for tumor necrosis factor. *J Immunol* **144**: 129–135.
- Selmaj K, Shafit-Zargardo B, Aquino DA, Farooq M, Raine CS, Norton WT, Brosnan CF (1991b). Tumor necrosis factor-induced proliferation of astrocytes from mature brain is associated with a down-regulation of glial fibrillary acidic protein mRNA. *J Neurochem* **57**: 823–830.
- Sengstock GJ, Zawia NH, Olanow CW, Dunn AJ, Arendash GW (1997). Intranigral iron infusions in the rat. Acute elevations in nigral lipid peroxidation and striatal dopaminergic markers with ensuing nigral degeneration. *Bio Trace Elem Res* **58**: 177–195.
- Shi B, DeGirolami U, Wang S, Lorenzo A, Busciglio J, Gabuzda D (1996). Apoptosis induced by HIV-infection of the central nervous system. *J Clin Invest* **98**: 1979–1990.
- Shoji Y, Uedono Y, Ishikura H, Takeyama N, Tanaka T (1995). DNA damage induced by tumour necrosis factor- α in L929 cells is mediated by mitochondrial oxygen radical formation. *Immunology* **84**: 543–548.
- Sloot WN, Gramsbergen JBP (1995). Detection of salicylate and its hydroxylated adducts 2,3- and 2,5-dihydroxybenzoic acids as possible indices for *in vivo* hydroxyl radical formation in combination with catechol- and indoleamines and their metabolites in cerebrospinal fluid and brain tissue. *J Neurosci Meth* **60**: 141–149.
- Smith TW, DeGirolami U, Henin D (1990). Human immunodeficiency virus (HIV) leukoencephalopathy and the microcirculation. *J Neuropathol Exp Neurol* **49**: 3357–3370.
- Streit WJ, Kincaid-Colton CA (1995). The brain's immune system. *Scientific Am* **11**: 54–61.
- Takahashi K, Wesselingh SL, Griffin DE, McArthur JC, Johnson RT, Glass JD (1996). Localization of HIV-1 in human brain using PCR/in situ hybridization and immunocytochemistry. *Ann Neurol* **39**: 705–711.
- Talley AK, Dewhurst S, Perry SW, Dollard SC, Gummuru S, Fine SM, New D, Epstein LG, Gendelman HE, Gelbard HA (1995). Tumor necrosis factor alpha-induced apoptosis in human neuronal cells: Protection by the antioxidant N-acetylcysteine and the genes bcl-2 and crmA. *Mol Cell Biol* **15**: 2359–2366.
- Tracey KJ, Cerami A (1993). Tumor necrosis factor: An updated review of its biology. *Crit Care Med* **21**: 415–422.
- Tross S, Price RW, Navia B, Thaler HT, Gold J, Hirsh DA, Sidtis JJ (1988). Neuropsychological characterization of the AIDS dementia complex: A preliminary report. *AIDS* **2**: 81–88.
- Wesselingh SL, Power C, Glass JD, Tyor WR, McArthur JC, Farber JM, Griffin JW, Griffin DE (1993). Intracerebral cytokine messenger RNA expression in acquired immunodeficiency syndrome dementia. *Ann Neurol* **33**: 576–582.
- Wiley CA, Schrier RD, Nelson JA, Lampert PW, Oldstone MBA (1986). Cellular localization of human immunodeficiency virus infection within the brains of acquired immunodeficiency syndrome patients. *Proc Natl Acad Sci USA* **83**: 7089–7093.
- Wilt SG, Milward E, Zhou JM, Nagasato K, Patton H, Rusten R, O'Connor M, Dubois-Dalcq M (1995). In vitro evidence for a dual role of tumor necrosis factor alpha in human immunodeficiency virus type 1 encephalopathy. *Ann Neurol* **37**: 381–394.